Research Article | **Open Access**

Nanosized TiO$_2$ Exposure Resulted in Neurotoxicity via Impairing NMDA Receptor-mediated Postsynaptic Signaling Cascade in Mice

Lei Sheng[1#], Ling Wang[2#], Yuguan Ze[1#], Xiaoyang Zhao[1#], Xiaohong Yu[1], Jie Hong[1], Dong Liu[1], Bingqing Xu[1], Xiaoyu Pan[1], Anan Lin[1], Yue Zhao[1], Chi Zhang[1], Yunting Zhu[1], Yi Long[1] and Fashui Hong[1*]

[1]Medical College of Soochow University, Suzhou 215123, China
[2]Library of Soochow University, Suzhou 215021, China
[#]equally to this work

Abstract

The central nervous system (CNS) toxicity induced by exposure to nano-sized particles is of great concern, but the mechanism of how this toxicity may be incurred has yet to be elucidated. Here, we examined how N-methyl-D-aspartate (NMDA) receptor-mediated postsynaptic signalling cascade may be affected by titanium dioxide particles (TiO$_2$ NPs) exposure for six consecutive months to contribute to the observed neurotoxicity. The results suggest that long-term exposure to TiO$_2$ NPs led to titanium accumulation and iron reduction in the blood and hippocampus tissues, and significant hippocampal injury as well as reduction of learning and memory in mice. The CNS injuries following long-term TiO$_2$ NP exposure were closely associated with significant reductions in NR1, NR2A, NR2B, calcium/calmodulin-dependent protein kinase II, postsynaptic density protein 95, nuclear activated extracellular-signal regulated kinase (ERK1/2), Dexras1, CAPON, peripheral benzodiazepine receptor-associated protein, and divalent metal transporter as well as elevation of synaptic Ras GTPase- activating protein and neural nitric oxide synthase in the hippocampus. It implies that long-term exposure to TiO$_2$ NPs may induce neurotoxic effects via impairing NMDA receptor-mediated postsynaptic signalling cascade in animals.

Keywords: Titanium dioxide nanoparticles; Hippocampus; N-methyl-D-aspartate receptors; Postsynaptic signalling proteins; Neurotoxicity

Introduction

Titanium dioxide nanoparticles (TiO$_2$ NPs) have been used in various areas, including pigment [1], paints [2], medicine [3], sunscreens [4], cosmetics[5], food additives and food packaging [6,7], and in environmental decontamination systems [8,9]. However, numerous studies demonstrated that TiO$_2$ NP exposure can conduct the damages of central nervous system (CNS) [10-17]. For instance, Wang et al. [12] indicated that TiO$_2$ NPs damaged CA1 region of the hippocampus and caused high inflammatory responses by elevating TNF-α and IL-1β levels, oxidative stress in the exposed mice [13]. Shin et al. [18] demonstrated that TiO$_2$ NPs induced TNF-α and IL-1β expression and enhanced nuclear factor-κB (NF-κB) binding activity by increasing microglial activation in the pre-inflamed brain of mice, and led to an exaggerated neuroinflammatory response. Our numerous studies suggested that exposure to TiO$_2$ NPs resulted in excessive species reactive oxygen (ROS) production and decreased antioxidant capacity[15], calcium overload, proliferation of glial cells, and altered contents trace elements neurotransmitters[19], led to hippocampal apoptosis via mitochondrial or the intrinsic pathway [16] and a reduction in spatial recognition memory in mice [16,19]. Furthermore, TiO$_2$ NP-induced oxidative damage in the mouse brain was demonstrated to be via the p38-Nrf-2 signaling pathway [20], and TiO$_2$ NP-induced neuroinflammation was associated with activation of the TLRs/TNF-α/NF-κB pathway [21]. However, the mechanisms of how this neurotoxicity are not understood.

N-methyl-D-aspartate receptors (NMDARs), which are glutamate-gated ion channel receptors, are widely expressed in the CNS and play pivotal roles in excitatory synaptic transmission, synaptic plasticity, learning and memory of mammalian brain [22]. NMDARs include different subunits within a repertoire of three subtypes: NR1, NR2 (NR2A-D) and NR3 (NR3A and NR3B) [23]; and NR1 and either NR2B or NR2A are most widely expressed [22]. Exposure to TiO$_2$ NPs was

demonstrated to increase glutamate release [19], and to inhibit NR2A and NR2B expression as well as to impair long-term potentiation (LTP) in rat or mouse hippocampus [24,25]. Therefore, we hypothesize that these changes mentioned above may further lead to the impairment of postsynaptic signalling cascade in the brain.

In excitatory synapses of the brain, specific receptors in the postsynaptic membrane can rapidly respond to the release of glutamate from the presynaptic terminal. Upon stimulation, these glutamate receptors activate postsynaptic signaling pathways that transduce signals into the postsynaptic neuron [26]. NMDAR activation can result in either LTP or long-term depression (LTD) of synaptic strength. NMDARs are embedded in the postsynaptic density (PSD), which involved in the postsynaptic membrane that contains a variety of scaffolding and signaling proteins. Many of the prominent proteins in the PSD fraction bind directly or indirectly to the NMDA receptor. Thus, the PSD fraction contains a core NMDA receptor-signaling complex, and serves as the signaling scaffold to bridge NMDARs to the intracellular signaling complexes [27-29] and is required to sustain the molecular organization of the postsynaptic density [30]. PSD-95 can also interact with a host of cytoplasmic signaling molecules, such as neuronal nitric oxide synthase (nNOS) and SynGAP, thereby connecting NMDARs to divergent signal transduction pathways [26]. Its overexpression can inhibit LTP and decrease LTD induction

[28,31,32]. Synaptic GTPase-activating protein (SynGAP) is a synaptic Ras GTPase-activating protein (RasGAP) that interacts with PSD-95 *in vitro* and *in vivo*. It stimulates GTPase activity of Ras, which shows that it negatively regulates Ras activity at excitatory synapses [33]. SynGAP was demonstrated to play a critical role in the regulation of neuronal mitogen-activated protein kinase (MAPK) signaling, α-amino-3-hydroxyl-5-methyl-4-isoxazole-proprionte glutamate receptor (AMPAR) membrane trafficking and excitatory synaptic transmission, and its overexpression led to a marked decrease of extracellular signal-regulated kinase (ERK) 1/2 activation [34]. While MAPK/ERK pathway plays a pivotal role in learning and memory [28,35,36]. In addition, NMDA receptor stimulation of nNOS activates Dexras1. Glutamate via NMDA receptors triggers cellular Ca^{2+} entry with calcium-calmodulin activating nNOS [37], whose binding to CAPON provides a mechanism for nitric oxide (NO) delivery to Dexras1, leading to S-nitrosylation of Dexras1 on cysteine-11 [38,39]. Therefore, the NMDA-NO-Dexras1-peripheral benzodiazepine receptor-associated protein (PAP7)-divalent metal transporter (DMT1)-iron uptake signaling cascade was suggested to mediate NMDA neurotoxicity [40]. Our previous study showed that TiO$_2$ NPs not only decreased expression of NR2A, NR2B, calcium/calmodulin-dependent protein kinase IV (CaMKIV), cyclic-AMP responsive element binding protein (CREB)-1, and CREB-2, and inhibited LTP [25], but also activated NOS and increased NO overproduction [15,19], and reduced iron content in mouse brain [19], these may interfere with the expression of NMDA receptor and postsynaptic signaling proteins mentioned above. However, the NMDA receptor-mediated postsynaptic signaling cascade caused by TiO$_2$ NPs in the hippocampus remains unclear.

In view of the above, the aim of the present study was to evaluate brain injury, and alterations in the expression of NR2A, NR2B, PSD-95, ERK1/2, SynGAP, Dexras1, CAPON, PAP7, nNOS, and DMT1 in mouse hippocampus, and to determine whether TiO$_2$ NP-induced neurotoxic effects via impairing NMDA receptor-mediated postsynaptic signaling cascade in the hippocampus caused by TiO$_2$ NP exposure.

Materials and Methods

Chemicals

Hydroxypropyl methylcellulose (HPMC) K4M was purchased from Sigma-Aldrich Company. Cell Lysis Kits were purchased from GENMED SCIENTICS INC (USA). Enzyme linked immunosorbent assay (ELISA) commercial kits were purchased from R&D Systems (USA). Other chemicals were purchased from Shanghai Chemical Co. (China).

The preparation, characteristics of TiO$_2$ NPs including the anatase structure, size, surface area, mean hydrodynamic diameter and ζ potential, have been described in our previous work [16,41]. X-ray-diffraction (XRD) were used to detect the anatase structure and size with a charge-coupled device (CCD) diffractometer (Mercury 3 Versatile CCD Detector; Rigaku Corporation, Tokyo, Japan) using Ni-filtered Cu Kα radiation. The NP size was determined using a TecnaiG220 transmission electron microscope (TEM) (FEI Co., USA). The surface area of NPs was determined by Brunauer–Emmett–Teller (BET) adsorption measurements on a Micromeritics ASCORBIC ACIDP 2020M+C instrument (Micromeritics Co., USA). The average aggregate or agglomerate size and ζ potential of NPs was measured by dynamic light scattering (DLS) using a Zeta PALS+BI-90 Plus (Brookhaven Instruments Corp., USA). XRD measurements suggested that TiO$_2$ NPs showed the anatase structure. The average particle size of powdered TiO$_2$ NPs suspended in 0.5% w/v HPMC solvent after 24 h

(5 mg/mL) incubation ranged from 5 to 6 nm, and the surface area was 174.8 m^2/g. The mean hydrodynamic diameter of TiO$_2$ NPs in HPMC solvent (5 mg/mL) ranged from 208 to 330 nm (mainly 294 nm), and the ζ potential after 24 h incubation was 9.28 mV [16].

Animals and treatment

One hundred and sixty CD-1 (ICR) female mice (24 ± 2 g) were purchased from the Animal Center of Soochow University (China). The mice were housed in stainless steel cages in a ventilated animal room. The room temperature in the housing facility was maintained at 24 ± 2°C, with a relative humidity of 60 ± 10% and a 12 h light/dark cycle. Distilled water and sterilized food were available *ad libitum*. Before treatment, the mice were acclimated to this environment for five days. All the animals were handled in accordance with the guidelines and protocols approved by the Care and Use of Animals Committee of Soochow University (China).

For the experiment, the mice were randomly divided into four groups (*N*=40 in each group), including a control group (treated with 0.5% w/v HPMC) and three experimental groups (1.25, 2.5, or 5 mg/kg BW TiO$_2$ NPs). The mice were weighed, volume of TiO$_2$ NP suspensions was calculated for each mouse, and the fresh TiO$_2$ NP suspensions were administered to the mice by nasal administration every day for 6 months. Any symptom or mortality was observed and recorded carefully everyday during the 6 months. In addition, the mice were regularly handled and weighed before the behavioral experiments.

Behavioral experiment

Following the 6 months of TiO$_2$ NP administration, the acquisition of spatial recognition memory was determined using the Y-maze in mice (*N*=10 in each group). In order to avoid any stress-related interference with the learning procedure, mice were not handled by the experimenter but were allowed to voluntarily enter the maze. To assess spatial recognition memory, the Y-maze test consisted of two trials separated by an intertrial interval (ITI). The Y-maze was consisted of three arms and was randomly designated: Start arm, in which the mouse started to explore (always open), Novel arm, which was blocked during the 1st trial, but open during the 2nd trial, and other arm (always open). The maze was placed in a sound attenuated room with dim illumination. The floor of the maze was covered with sawdust, which was mixed after each individual trial in order to eliminate olfactory stimuli. Visual cues were placed on the walls of the maze, and the observer was always in the same position at least 3 m from the maze. Assay of acquisition of spatial recognition memory in mice was described in previous reports [42,43].

To measure spatial recognition memory, the number of entries and time spent in each arm of the maze by each mouse was recorded and novelty versus familiarity was analyzed by comparing behavior in all three arms. The number of arms visited was taken as an indicator of locomotor and exploratory activity.

Preparation of hippocampus

After behavioral detection, mice were weighed. Blood samples were collected from the eye vein by rapidly removing the eyeball. The hippocampi from all animals were quickly dissected from brains and placed in ice-cold dish.

Analysis of titanium and iron content

The hippocampi were thawed and approximately 0.1 g samples were weighed, then these tissues and 5 ml blood were digested, and analyzed for titanium, and iron content (*N*=5 in each group). Briefly,

prior to elemental analysis, the blood and hippocampal tissues were digested overnight with nitric acid (ultrapure grade). After adding 0.5 mL of H_2O_2, the mixed solutions were incubated at 160°C in high pressure reaction containers in an oven until the samples were completely digested. Then, the solutions were incubated at 120°C to remove any remaining nitric acid until the solutions were colorless and clear. Finally, the remaining solutions were diluted to 3 mL with 2% nitric acid. Inductively coupled plasma-mass spectrometry (Thermo Elemental X7; Thermo Electron Co., Waltham, MA, USA) was used to determine the titanium, and iron concentration in the samples. Indium of 20 ng/mL was chosen as an internal standard element. The detection limit of titanium, and iron was 0.089 ng/mL, and 0.062 ng/mL, respectively.

Histopathological examination

For pathologic studies, all histopathologic examinations were performed using standard laboratory procedures. Briefly, hippocampi ($N=5$ in each group) were embedded in paraffin blocks, then sliced (5 μm thickness) and placed onto glass slides. After hematoxylin–eosin staining, the stained sections were evaluated by a histopathologist unaware of the treatments, using an optical microscope (Nikon U-III Multi-point Sensor System, Japan).

Assay of gene and protein expression

The levels of mRNA expression of *NR1, NR2A, NR2B, CaMKII, PSD-95, SynGAP, ERK1/2, Dexras1, CAPON, PAP7, DMT1,* and *nNOS* in the hippocampi were determined using real-time quantitative RT polymerase chain reaction (RT-PCR) ($N=5$ in each group) [44-46]. Synthesized cDNA was used for the real-time PCR. Primers were designed using Primer Express Software according to the software guidelines (Table 1). Total RNA was extracted from individual hippocampi using from the homogenates was isolated using Tripure

Isolation Reagent (Roche, USA) according to the manufacturer's instructions. The RT reagent (Shinegene Co., China) of 30 μl was prepared by mixing 15 μl of 2×RT buffer, 1 l random primer in a concentration of 100 pmol.μl⁻¹, 1μl of RTase, 5 μl RNA, and 8 μl DEPC water together. The reaction condition was 25°C for 10 min, 40°C for 60 min, and 70°C for 10 min. The internal reference gene was actin3. qRT-PCR was performed using the 7500 Real-time PCR System (ABI) with SYBR Premix Ex Taq™ (Takara) according to the manufacturer's instructions. The RT-qPCR data were processed with the sequence detection software version 1.3.1 following the method of Schefe et al. [47], analyzed based on the standard curve using the threshold cycle (Ct) model for relative quantification [45] and the expression levels of mRNA of all genes were normalized by the contents of actins mRNAs.

To determine protein levels of NR1, NR2A, NR2B, CaMKII, PSD-95, SynGAP, ERK1/2, Dexras1, CAPON, PAP7, DMT1, and nNOS in the hippocampi, total protein from the frozen hippocampal tissues ($N=5$ in each group) from experimental and control mice was extracted using Cell Lysis Kits (GENMED SCIENTIFICS INC.USA) and quantified using BCA protein assay kits (GENMED SCIENTIFICS INC.USA). ELISA was performed using commercial kits that were selective for each respective protein (R&D Systems, USA), following the manufacturer's instructions. The absorbance was measured on a microplate reader at 450 nm (Varioskan Flash, Thermo Electron, Finland), and the concentrations of NR1, NR2A, NR2B, CaMKII, PSD-95, SynGAP, ERK1/2, Dexras1, CAPON, PAP7, DMT1, and nNOS were calculated from a standard curve for each sample.

Statistical analysis

All results are expressed as means ± SD. The Kolmogorov-Smirnov test with Dunn's post test was used to compare control and treated groups using SPSS 19 software (SPSS, Inc., Chicago, IL, USA). A P-value<0.05 was considered statistically significant.

Gene name	Description	Primer sequence	Primer size (bp)
Refer-actin	mactin-F	5'-GAGACCTTCAACACCCCAGC-3'	
	mactin-R	5'-ATGTCACGCACGATTTCCC-3'	263
NR1	mNR1-F	5'-CAGTGCCCCAGTGCTGTTAT-3'	
	mNR1- R	5'-CTCTCCCATCATTCCGTTCC-3'	164
NR2A	mNR2A F	ATGAACCGCACTGACCCTAAG	
	mNR2A R	GGCTTGCTGCTGGATGGA	246
NR2B	mNR2B F	AATGTGGATTGGGAGGATAGG	
	mNR2B R	ATTAGTCGGGCTTTGAGGATACT	255
CaMKII	mCaMKII -F	5'- AGTCCAGTTCCAGCGTTCAGT -3'	
	mCaMKII -R	5'- GGGTCGCACATCTTCGTGTA -3'	166
PSD-95	mPSD-95-F	5'-GTTCCCCGACAAGTTTGGAT-3'	
	mPSD-95-R	5'-CTCGCACAGACTGGACGCT-3'	191
SynGAP	mSynGAP-F	5'-ATCCACGCTTAACCCCACA-3'	
	mSynGAP-R	5'-CTCATACTCCTTCACCCTGTCC-3'	175
ERK1/2 (Mapk1)	mERK1/2-F	5'-GCACCGTGACCTCAAGCC-3'	
	mERK1/2-R	5'-TGCAGCCCACAGACCAAA-3'	212
Dexras1	mDexras1-F	5'-CCATCGAGGACTTCCACCG-3'	
	mDexras1-R	5'-GCTGAACACCAGAATGAAAACG-3'	146
CAPON	mCAPON-F	5'-ACAGACATTGACGCCGTGG-3'	
	mCAPON-R	5'-TCCTGAGGGTGGGGTGAGA-3'	137
PAP7	mPAP7-F	5'-GAGAAGTCGTCACCGTCCG-3'	
	mPAP7-R	5'-AAATAAACCCCAAACCCAATG-3'	100
nNOS	mnNOS-F	5'-CGCTGCTACAACCTCGCTAC-3'	
	mnNOS-R	5'-TGAGCCAGGAGGAGCACAC-3'	144
DMT1	mDMT1-F	5'-TCACCATCGCAGACACTTTTG-3'	
	mDMT1-R	5'-GACAGGACGGCACGAACAT-3'	174

Table 1: Real time PCR primer pairs. PCR primers used in the gene expression analysis.

Percentage of duration of visits(%)	Control	1.25 mg/kg	2.5 mg/kg	5 mg/kg
Novel arm	44 ± 5.5	30 ± 4.2*	16 ± 2.8**	6 ± 1.7***
Start arm	26.5 ± 2.9	32 ± 4.1*	38 ± 5.7*	42 ± 5.9**
Other arm	29.5 ± 3.3	38 ± 5.1*	46 ± 6.6**	52 ± 7.8**

*$p < 0.05$, and **$p<0.01$. Values represent means ± SD (N=10).

Table 2: Effect of TiO$_2$ NPs on the spatial recognition memory of mice in Y-maze after nasal administration of TiO$_2$ NPs for six consecutive months.
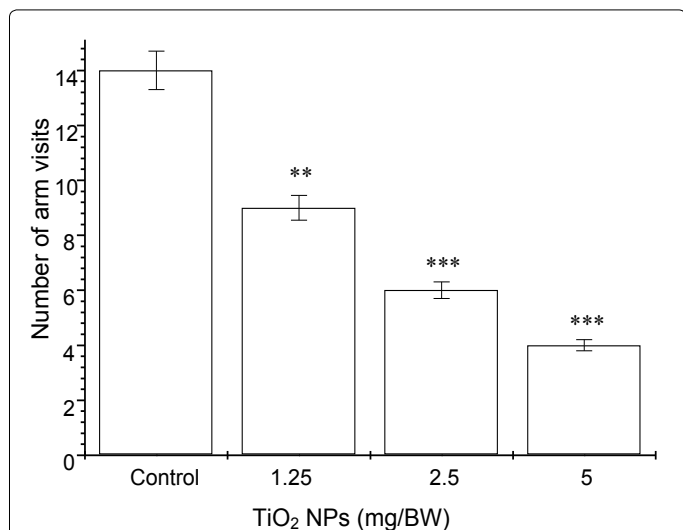

Figure 1: Effects of TiO$_2$ NPs on locomotor activity of mice in Y-maze after nasal administration of TiO$_2$ NPs for six consecutive months. **$p<0.01$, and ***$p<0.01$. Values represent means ± D (*N=10*).
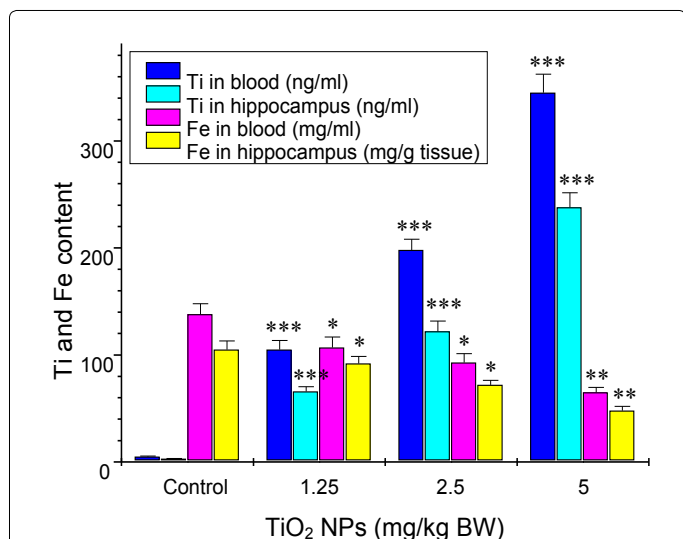

Figure 2: Titanium and iron contents in the blood and hippocampus of mice after nasal administration of TiO$_2$ NPs for six consecutive months. *$p<0.05$, **$p<0.01$, and ***$p<0.01$. Values represent means ± SD (*N=5*).

Results

Spatial recognition memory and locomotor activity

Table 2 exhibits effects of TiO$_2$ NPs on the spatial recognition memory of mice. It can be observed that the percentage duration in the novel arm in control mice was significantly higher than that in the

start and other arms, whereas the percentage duration in the novel arm in 1.25, 2.5, or 5 mg/kg BW TiO$_2$ NP-exposed mice was significantly decreased as compared to the control mice throughout the experiment ($P<0.05$), respectively, suggesting that long-term exposure to TiO$_2$ NPs reduced leaning and memory of mice. To confirm effects of TiO$_2$ NPs on locomotor activity of mice, number of arm visits was also examined and are presented in Figure 1. With increased TiO$_2$ NP dose, the number of arm entries markedly decreased ($P<0.05$).

Titanium and iron contents

Figure 2 presents titanium and iron contents in the blood and hipocampus caused by TiO$_2$ NP exposure. With increased TiO$_2$ NP dose, there were significant increases of titanium levels, whereas iron levels were markedly reduced in the blood and hipocampus (Figure 2, $P<0.01$). Titanium content in the control mice was negligent (Figure 2). The increased titanium and decreased iron may lead to hippocampal injury and impairment of hippocampal function, which were confirmed by the assays of NMDA receptor and postsynaptic signalling factors as well as histopathological observations of mouse hippocampus.

Hippocampal histopathological observations

Following long-term exposure to 1.25, 2.5, or 5 mg/kg BW TiO$_2$ NPs, histopathological changes from hippocampal CA region were observed (Figure 3B-3D), which suggested significant edema of glial cells, disperative replication of neuron cells, decreased size of cell volume, nuclear irregularity, and necrosis or abscission of neuron cells.

Expression of NMDA receptor subunit and postsynaptic signaling factor

In the present study, actin3 was chosen as the endogenous control gene. The expression level of the actin3 gene was constant, with an
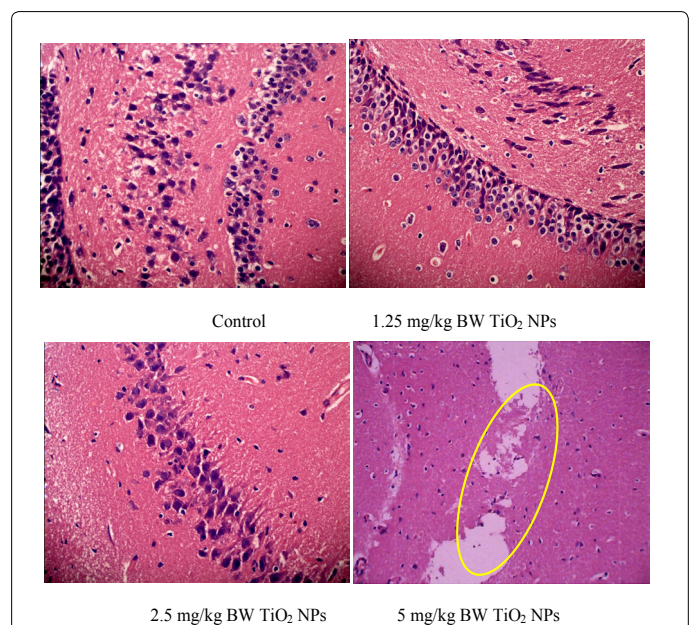

Control   1.25 mg/kg BW TiO$_2$ NPs

2.5 mg/kg BW TiO$_2$ NPs   5 mg/kg BW TiO$_2$ NPs

Figure 3: Histopathology of CA region of hippocampus in mice after nasal administration of TiO2 NPs for six consecutive months. (a) Control group indicates great nucleus and limpid nucleolus of glial cells and pyramidal cells; (b) 1.25 mg/kg BW TiO$_2$ NP group indicates disperative replication of pyramidal cells, edema of glial cells; (c) 2.5 mg/kg BW TiO$_2$ NP group indicates disperative replication of pyramidal cells, decreased size of cell volume, nuclear irregularity; (d) 5 mg/kg BW TiO$_2$ NP group indicates degeneration, necrosis or abscission of neuron cells.

Ratio of gene/actin (Fold)	Control	1.25 mg/kg	2.5 mg/kg	5 mg/kg
NR1	1.02 ± 0.15	0.85 ± 0.11	0.36 ± 0.06**	0.25 ± 0.04**
NR2A	0.84 ± 0.09	0.55 ± 0.06*	0.27 ± 0.03**	0.21 ± 0.02**
NR2B	0.68 ± 0.07	0.45 ± 0.04*	0.29 ± 0.04**	0.18 ± 0.02***
CaMKII	1.13 ± 0.15	0.88 ± 0.12	0.49 ± 0.05**	0.31 ± 0.03***
PSD-95	0.72 ± 0.08	0.47 ± 0.05*	0.32 ± 0.03**	0.21 ± 0.01***
SynGAP	0.37 ± 0.02	0.62 ± 0.04*	0.81 ± 0.06*	0.98 ± 0.09**
ERK1/2(Mapk1)	4.57 ± 0.35	2.96 ± 0.24*	2.44 ± 0.22*	1.84 ± 0.19**
Dexras1	3.94 ± 0.29	2.46 ± 0.21*	1.56 ± 0.18**	1.01 ± 0.12***
CAPON	0.67 ± 0.08	0.42 ± 0.05*	0.34 ± 0.03**	0.25 ± 0.02**
PAP7	1.27 ± 0.13	0.75 ± 0.08*	0.42 ± 0.04**	0.21 ± 0.02***
nNOS	3.72 ± 0.31	5.05 ± 0.46*	6.39 ± 0.57*	10.56 ± 1.08***
DMT1	0.85 ± 0.07	0.54 ± 0.05*	0.36 ± 0.04**	0.22 ± 0.02***

*$p < 0.05$, **$p < 0.01$, and ***$p < 0.01$. Values represent means ± SD (N=5).

Table 3: Effect of TiO₂ NPs on mRNA expression of gene in mouse hippocampus after nasal administration of TiO₂ NPs for six consecutive months.

Protein expression (ng/g tissue)	Control	1.25 mg/kg	2.5 mg/kg	5 mg/kg
NR1	58.14 ± 3.91	49.05 ± 3.55	18.72 ± 1.93**	12.75 ± 1.52***
NR2A	49.56 ± 3.55	29.15 ± 2.46*	14.04 ± 1.52**	10.71 ± 1.25***
NR2B	40.12 ± 3.62	33.85 ± 2.5	15.08 ± 1.85**	9.18 ± 1.21***
CaMKII	67.88 ± 5.12	56.64 ± 5.05	25.48 ± 2.27**	15.81 ± 1.32***
PSD-95	43.25 ± 3.61	24.91 ± 2.26*	16.64 ± 1.42**	10.71 ± 1.05***
SynGAP	18.53 ± 1.62	32.24 ± 2.83*	43.74 ± 3.58*	54.88 ± 4.89***
ERK1/2	182.86 ± 12.31	115.44 ± 8.51*	92.72 ± 6.36*	64.69 ± 5.33**
Dexras1	236.48 ± 16.58	159.96 ± 11.26*	96.72 ± 8.85**	58.58 ± 6.39***
CAPON	40.22 ± 3.21	27.31 ± 2.36*	21.08 ± 2.23*	14.56 ± 1.38**
PAP7	76.28 ± 5.85	48.75 ± 3.27*	26.04 ± 2.31**	12.18 ± 1.18***
nNOS	212.04 ± 13.62	257.95 ± 15.89	389.79 ± 25.68**	654.72 ± 45.71***
DMT1	51.55 ± 4.71	43.78 ± 3.59	19.88 ± 2.09**	12.98 ± 1.04***

*$p < 0.05$, **$p < 0.01$, and ***$p < 0.01$. Values represent means ± SD (N=5).

Table 4: Effect of TiO₂ NPs on levels of protein expression of gene in mouse hippocampus after nasal administration of TiO₂ NPs for six consecutive months.

expression ratio of almost one in all the samples (data not listed). Therefore, using this gene as a reference, changes in the expression levels of the 12 NMDA receptor subunit and/or postsynaptic signaling factor genes were evaluated and compared following exposure to TiO₂ NPs for six consecutive months (Table 3).

Long-term exposure to TiO₂ NPs resulted in a dose-dependent marked decrease in the mRNA and protein expression of NMDA receptor subunits, including NR1, NR2A and NR2B in the hippocampus (Tables 3 and 4), suggesting reductions of 16.67%, 64.71% and 75.49%; 15.63%, 67.8% and 78.07% for NR1; reductions of 34.52%, 67.85% and 75%; 41.18%, 71.67% and 78.39% for NR2A, reductions of 33.82%, 57.35% and 73.53%; 15.63%, 62.41% and 77.11% for NR2B, respectively.

To confirm NMDA receptor-mediated postsynaptic signaling cascade, the levels of several postsynaptic signaling factors, including CaMKII, PSD-95, SynGAP, ERK1/2, Dexras1, CAPON, PAP7, DMT1, and nNOS in mouse hippocampus, were analyzed by RT-PCR and ELISA. As the dose of TiO₂ NPs increased, there were significant reductions in CaMKII, PSD-95, ERK1/2, Dexras1, CAPON, PAP7, and DMT1 expression; whereas there were marked increases of SynGAP and nNOS expression in the hippocampi (Tables 3 and 4, $P < 0.05$).

Discussion

In the current study, the effects of long-term exposure to TiO₂ NPs on the expression of NMDA receptor and postsynaptic signalling factors in mouse hippocampus were evaluated. The TiO₂ NP accumulation was confirmed by the markedly increased titanium levels in the blood and hippocampus (Figure 2), suggesting that TiO₂ NPs can easily cross blood-brain barrier into the hippocampus, depositing TiO₂ NPs in the hippocampus (Figure 2) and damaging hippocampus (Figure 3). In addition, TiO₂ NP exposure resulted in reductions of iron contents in the blood and hippocampus (Figure 2). Our previous study has been demonstrated that exposed mice to TiO₂ NPs presented low iron content [20]. Numerous studies demonstrated that TiO₂ NP accumulation and iron deficiency in mouse brain resulted in excessive production of species reactive oxygen (ROS), and increased peroxidation levels [15-17,19,48-50], which may damage hippocampus. The Y maze is regarded as one of common behavioral tasks to evaluate cognitive abilities of rodents. Hippocampus-dependent spatial learning and memory are frequently investigated by observing the behavioral performance of animals in the Y maze. The results of this study indicated that long-term exposure to TiO₂ NPs resulted in decreases in spatial recognition memory (Table 2), for example, the time spent in the unfamiliar novel arm in the TiO₂ NP-exposed mice was lower than unexposed mice (Table 2). Locomotor activity acts as a function of the excitability level of the CNS [51]. The present study shows that TiO₂ NP exposure for six consecutive months decreased locomotor activity in mice (Figure 1), which is consistent with our previous reports [15-17,19-21,25]. Decreased spatial cognition of mice caused by TiO₂ NP exposure may be closely associated with the accumulation of TiO₂ NPs, reduction of iron uptake and the damaged hippocampus. Furthermore, decreased spatial cognition of mice may be triggered through NMDA receptor-mediated postsynaptic signaling cascade in the hippocampus.

The present study shows that long-term exposure to TiO₂ NPs significantly decreased NR1, NR2A and NR2B in the hippocampus

(Tables 3 and 4), which is consistent with our previously reported results [25]. This finding supports our assumed alteration of NMDA receptor in the TiO$_2$ NP-exposed mice. Numerous important NMDA receptor properties are influenced by the subunits composing the receptor assembly [52]. It was reported that LTP in the hippocampus is specifically related to NR2A-containing NMDARs [53]. TiO$_2$ NP exposure was suggested to markedly inhibit the induction and establishment of LTP in rats and mice [24,25]. Alteration of NMDA receptor expression may affect expression of postsynaptic signaling factors. Upon NMDA receptor stimulation, CaMKII is endlessly induced and is essential for NMDAR-dependent LTP [54]. CaMKII expression has been demonstrated to play an important role in learning, memory, and synaptic plasticity [55]. Toscano et al. [56] demonstrated that Pb^{2+} exposure could decrease CaMKII activity and expression in rats. In current study, reduced NR1, NR2A and NR2B and CaMKII expression were found in the TiO$_2$ NP-exposed mice, suggesting that TiO$_2$ NPs may disrupt the normal NMDA receptor assembly and the function of CaMKII. Our previous finding also indicated that TiO$_2$ NP exposure led to reductions of CaMKIV activity and expression, spatial cognition, and synaptic plasticity in mice [25]. As a signaling scaffold, PSD-95 brings intracellular signaling complexes close to NMDAR channels. PSD-95 bridges the Ca^{2+} influx to the specific downstream signaling events [29]. Our data suggest that with increased TiO$_2$ NP dose, decreased PSD-95 expression in the hippocampus was significantly observed (Tables 3 and 4), which would impair the molecular organization of the postsynaptic density, synaptic strength and plasticity [30]. SynGAP had been demonstrated to be a negative regulator of Ras at excitatory synapses [33], and to be inhibited by CaMKII phosphorylation [57]. Furthermore, ERK activation had been suggested to play an important role in the consolidation and reconsolidation of recognition memory [58]. In the present study, our data show that TiO$_2$ NP exposure significantly reduced CaMKII expression and increased SynGAP expression, leading the inhibition of ERK1/2 expression in mouse hippocampus (Tables 3 and 4).

Nitric oxide (NO) may not freely diffuse to reach its physiological targets but may be conveyed to these sites by interactions of NOS with other proteins [40]. As shown by reports, nNOS can bind to the PSD-95/93, which in turn binds to NMDA receptors [59,60]. This ternary complex enables NO to S-nitrosylate NMDA receptors and alters their signaling [61]. Therefore, we presume that increased nNOS expression and decreased PSD-95 expression caused by TiO$_2$ NPs may influence NO to S-nitrosylate NMDA receptors and interfere their signaling in the hippocampus.

CAPON was identified to be a 55 kDa protein that contains a C-terminal domain that binds to the PDZ domain of nNOS and an N-terminal phosphotyrosine binding (PTB) domain [38], and interacts with Dexras1 [40,62,63]. While Dexras1 shares about 35% homology with the Ras subfamily of proteins and contains all of the conserved domains of typical GTPases, and has also been designated activator of G protein signaling 1 (AGS1) or RASD1 [40,64], activating extracellular signal-regulated kinases 1, 2 (ERK1, 2) [65-67]. PAP7 is proved to bind to DMT1, the only known physiological import channel for iron, activation of NMDA receptor stimulates nNOS, resulting in S-nitrosylation and activation of Dexras1, which induces iron uptake via interactions with PAP7 and DMT1. Glutamate, acting via NMDA receptors, activates nNOS to form NO [37], which leads to protein S-nitrosylation [68]. This modification activates Dexras1, which, by its link to PAP7, augments both Tf-mediated and NTBI uptake. From Figure 3, we observed a marked reduction of the Fe content in the TiO$_2$ NP-exposed hippocampus. The roles of intraneuronal iron are involved in synthesis, packaging of neurotransmitters, uptake as well as degradation of the neurotransmitters into other iron-containing proteins that may directly or indirectly alter brain function through peroxide reduction, amino acid metabolism and fat desaturation, thus changing postsynaptic membrane functioning [69]. In the present study, long-term exposure to TiO$_2$ NPs significantly decreased levels of ERK1/2, Dexras1, CAPON, PAP7, and DMT1 expressions and elevated nNOS level (Tables 3 and 4), which may be associated with reduction of iron uptake (Figure 2), thus impairing NMDA-NO-Dexras1-PAP7-DMT1-iron uptake postsynaptic signaling cascade in the hippocampus [70].

Conclusion

Mice were exposed to TiO$_2$ NPs for six consecutive months, titanium accumulation and iron reduction in the blood and hippocampus tissues were observed, which in turn resulted in significant hippocampal injury and reduction of spatial cognition in mice. The CNS injuries following long-term TiO$_2$ NP exposure may be closely associated with NMDA receptor-mediated postsynaptic signaling cascade, marked by significant reductions in NR1, NR2A, NR2B, CaMKII, PSD-95, ERK1/2, Dexras1, CAPON, PAP7, and DMT1 expressions as well as elevations of SynGAP and nNOS expressions in the hippocampus. Therefore, the application of TiO$_2$ NPs should be carried out cautiously, especially in humans.

References

1. Pfaff G, Reynders P (1999) Angle-Dependent Optical Effects Deriving from Submicron Structures of Films and Pigments. Chem Rev 99: 1963-1982.

2. Braun JH, Baidins A, Marganski RE (1992) Preparation of TiO$_2$ porous films by anodization. Prog Org Coat 20:105-138.

3. Skocaj M, Filipic M, Petkovic J, Novak S (2011) Titanium dioxide in our everyday life; is it safe? Radiol Oncol 45: 227-247.

4. Zallen R, Moret MP (2006) The optical absorption edge of brookite TiO$_2$. Solid State Commun 137: 154-157.

5. Kaida T, Kobayashi K, Adachi M, Suzuki F (2004) Optical characteristics of titanium oxide interference film and the film laminated with oxides and their applications for cosmetics. J Cosmet Sci 55: 219-220.

6. Fayaz AM, Balaji K, Girilal M, Kalaichelvan PT, Venkatesan R (2009) Mycobased synthesis of silver nanoparticles and their incorporation into sodium alginate films for vegetable and fruit preservation. J Agric Food Chem 57: 6246- 6252.

7. Lopez-Moreno ML, De La Rosa G, Hernandez-Viezcas JA, Peralta-Videa JR, Gardea-Torresdey JL (2010) X-ray absorption spectroscopy (XAS) corroboration of the uptake and storage of CeO2 nanoparticles and assessment of their differential toxicity in four hdible plant species. J Agric Food Chem 58: 3689-3693.

8. Esterkin CR, Negro AC, Alfano OM, Cassano AE (2005) Air pollution remediation in a fixed bed photocatalytic reactor coated with TiO$_2$. AIChE J 51: 2298–2310.

9. Choi H, Stathatos E, Dionysiou D (2006) Sol–gel preparation of mesoporous photocatalytic TiO$_2$ films and TiO2/Al2O3 composite membranes for environmental applications. Appl Catal B – Environ 63: 60-67.

10. Long TC, Saleh N, Tilton RD, Lowry G, Veronesi B (2006) Titanium dioxide (P25) produces reactive oxygen species in immortalized brain microglia (BV2): implications for nanoparticle neurotoxicity. Environ Sci Technol 40: 4346–4352.

11. Long TC, Tajuba J, Sama P, Saleh N, Swartz C, et al. (2007) Nanosize titanium dioxide stimulates reactive oxygen species in brain microglia and damages neurons in vitro. Environ Health Perspect 115: 1631-1637.

12. Wang J, Chen C, Liu Y, Jiao F, Li W, et al. (2008) Potential neurological lesion after nasal instillation of TiO(2) nanoparticles in the anatase and rutile crystal phases. Toxicol Lett 183: 72-80.

13. Wang J, Liu Y, Jiao F, Lao F, Li W, et al. (2008) Time-dependent translocation and potential impairment on central nervous system by intranasally instilled TiO(2) nanoparticles. Toxicology 254: 82-90.

14. Shimizu M, Tainaka H, Oba T, Mizuo K, Umezawa M, et al. (2009) Maternal exposure to nanoparticulate titanium dioxide during the prenatal period alters gene expression related to brain development in the mouse. Part Fibre Toxicol 6: 20.

15. Ma L, Liu J, Li N, Wang J, Duan Y, et al. (2010) Oxidative stress in the brain of mice caused by translocated nanoparticulate TiO$_2$ delivered to the abdominal cavity. Biomaterials 31: 99-105.

16. Hu R, Zheng L, Zhang T, Gao G, Cui Y, et al. (2011) Molecular mechanism of hippocampal apoptosis of mice following exposure to titanium dioxide nanoparticles. J Hazard Mater 191: 32-40.

17. Ze Y, Hu R, Wang X, Sang X, Ze X, et al. (2014) Neurotoxicity and gene-expressed profile in brain-injured mice caused by exposure to titanium dioxide nanoparticles. J Biomed Mater Res A 102: 470-478.

18. Shin JA, Lee EJ, Seo SM, Kim HS, Kang JL, et al. (2010) Nanosized titanium dioxide enhanced inflammatory responses in the septic brain of mouse. Neuroscience 165: 445-454.

19. Hu R, Gong X, Duan Y, Li N, Che Y, et al. (2010) Neurotoxicological effects and the impairment of spatial recognition memory in mice caused by exposure to TiO2 nanoparticles. Biomaterials 31: 8043-8050.

20. Ze YG, Zheng L, Zhao XY, Gui SX, Sang XZ, et al. (2012) Molecular mechanism of titanium dioxide nanoparticles-induced oxidative injury in the brain of mice. Chemosphere 92: 1183-1189.

21. Ze Y, Sheng L, Zhao X, Hong J, Ze X, et al. (2014) TiO2 nanoparticles induced hippocampal neuroinflammation in mice. PLoS One 9: e92230.

22. Papadia S, Hardingham GE (2007) The dichotomy of NMDA receptor signaling. Neuroscientist 13: 572-579.

23. Paoletti P, Neyton J (2007) NMDA receptor subunits: function and pharmacology. Curr Opin Pharmacol 7: 39-47.

24. Gao X, Yin S, Tang M, Chen J, Yang Z, et al. (2011) Effects of developmental exposure to TiO$_2$ nanoparticles on synaptic plasticity in hippocampal dentate gyrus area: an in vivo study in anesthetized rats. Biol Trace Elem Res 143: 1616-1628.

25. Ze YG, Sheng L, Zhao XY, Ze X, Wang XC, et al. (2014) Neurotoxic characteristics of spatial recognition damage of the hippocampus in mice following subchronic peroral exposure to TiO$_2$ nanoparticles. J Hazard Mater 264: 219–229.

26. Sheng M, Kim MJ (2002) Postsynaptic signaling and plasticity mechanisms. Science 298: 776-780.

27. Kennedy MB (2000) Signal-processing machines at the postsynaptic density. Science 290: 750-754.

28. Luo JH, Qiu ZQ, Zhang L, Shu WQ (2012) Arsenite exposure altered the expression of NMDA receptor and postsynaptic signaling proteins in rat hippocampus. Toxicol Lett 211: 39-44.

29. Xu W (2011) PSD-95-like membrane associated guanylate kinases (PSD-MAGUKs) and synaptic plasticity. Curr Opin Neurobiol 21: 306-312.

30. Chen X, Nelson CD, Li X, Winters CA, Azzam R, et al. (2011) PSD-95 is required to sustain the molecular organization of the postsynaptic density. J Neurosci 31: 6329-6338.

31. Béïque JC, Andrade R (2003) PSD-95 regulates synaptic transmission and plasticity in rat cerebral cortex. J Physiol 546: 859-867.

32. Stein V, House DR, Bredt DS, Nicoll RA (2003) Postsynaptic density-95 mimics and occludes hippocampal long-term potentiation and enhances long-term depression. J Neurosci 23: 5503-5506.

33. Kim JH, Liao D, Lau LF, Huganir RL (1998) SynGAP: a synaptic RasGAP that associates with the PSD-95/SAP90 protein family. Neuron 20: 683-691.

34. Rumbaugh G, Adams JP, Kim JH, Huganir RL (2006) SynGAP regulates synaptic strength and mitogen-activated protein kinases in cultured neurons. Proc Natl Acad Sci U S A 103: 4344-4351.

35. Schaeffer HJ, Weber MJ (1999) Mitogen-activated protein kinases: specific messages from ubiquitous messengers. Mol Cell Biol 19: 2435-2444.

36. Sweatt JD (2004) Mitogen-activated protein kinases in synaptic plasticity and memory. Curr Opin Neurobiol 14: 311-317.

37. Bredt DS, Snyder SH (1994) Nitric oxide: a physiologic messenger molecule. Annu Rev Biochem 63: 175-195.

38. Jaffrey SR, Snowman AM, Eliasson MJ, Cohen NA, Snyder SH (1998) CAPON: a protein associated with neuronal nitric oxide synthase that regulates its interactions with PSD95. Neuron 20: 115-124.

39. Jaffrey SR, Fang M, Snyder SH (2002) Nitrosopeptide mapping: a novel methodology reveals s-nitrosylation of dexras1 on a single cysteine residue. Chem Biol 9: 1329-1335.

40. Cheah JH, Kim SF, Hester LD, Clancy KW, Patterson SE 3rd, et al. (2006) NMDA receptor-nitric oxide transmission mediates neuronal iron homeostasis via the GTPase Dexras1. Neuron 51: 431-440.

41. Yang P, Lu C, Hua N, Du Y (2002) Titanium dioxide nanoparticles co-doped with Fe^{3+} and Eu^{3+} ions for photocatalysis. Mater Lett 57: 794–801.

42. Akwa Y, Ladurelle N, Covey DF, Baulieu EE (2001) The synthetic enantiomer of pregnenolone sulfate is very active on memory in rats and mice, even more so than its physiological neurosteroid counterpart: distinct mechanisms? Proc Natl Acad Sci U S A 98: 14033-14037.

43. Dellu F, Contarino A, Simon H, Koob GF, Gold LH (2000) Genetic differences in response to novelty and spatial memory using a two-trial recognition task in mice. Neurobiol Learn Mem 73: 31-48.

44. Ke LD, Chen Z, Yung WK (2000) A reliability test of standard-based quantitative PCR: exogenous vs endogenous standards. Mol Cell Probes 14: 127-135.

45. Livak KJ, Schmittgen TD (2001) Analysis of relative gene expression data using real-time quantitative PCR and the 2(-Delta Delta C(T)) Method. Methods 25: 402-408.

46. Liu W, Saint DA (2002) Validation of a quantitative method for real time PCR kinetics. Biochem Biophys Res Commun 294: 347-353.

47. Schefe JH, Lehmann KE, Buschmann IR, Unger T, Funke-Kaiser H (2006) Quantitative real-time RT-PCR data analysis: current concepts and the novel "gene expression's CT difference" formula. J Mol Med (Berl) 84: 901-910.

48. Rao R, de Ungria M, Sullivan D, Wu P, Wobken JD, et al. (1999) Perinatal brain iron deficiency increases the vulnerability of rat hippocampus to hypoxic ischemic insult. J Nutr 129: 199-206.

49. John LB (2001) Iron-deficiency anemia: examining the nature and magnitude of the public health problem. J Nutr 131: 568s-580s.

50. Patel BN, Dunn RJ, Jeong SY, Zhu QZ, Julien JP, et al. (2002) Ceruloplasmin regulates iron levels in the CNS and prevents free radical injury. J Neurosci 22: 6578- 6586.

51. Masur J, Märtz RM, Carlini EA (1971) Effects of acute and chronic administration of cannabis sativa and (-) delta9-trans-tetrahydrocannabinol on the behavior of rats in an open-field arena. Psychopharmacologia 19: 388-397.

52. Cull-Candy SG, Brickley SG (2001) NMDA Receptors. Encyclopedia of Life Sciences Nature Publishing Group, pp. 1–8.

53. Liu L, Wong TP, Pozza MF, Lingenhoehl K, Wang Y, et al. (2004) Role of NMDA receptor subtypes in governing the direction of hippocampal synaptic plasticity. Science 304: 1021-1024.

54. Lisman J, Schulman H, Cline H (2002) The molecular basis of CaMKII function in synaptic and behavioural memory. Nat Rev Neurosci 3: 175-190.

55. Hardingham N, Glazewski S, Pakhotin P, Mizuno K, Chapman PF, et al. (2003) Neocortical long-term potentiation and experience-dependent synaptic plasticity require alpha-calcium/calmodulin-dependent protein kinase II autophosphorylation. J Neurosci 23: 4428-4436.

56. Toscano CD, O'Callaghan JP, Guilarte TR (2005) Calcium/calmodulin-dependent protein kinase II activity and expression are altered in the hippocampus of Pb^{2+}-exposed rats. Brain Res 1044: 51-58.

57. Chen HJ, Rojas-Soto M, Oguni A, Kennedy MB (1998) A synaptic Ras-GTPase activating protein (p135 SynGAP) inhibited by CaM kinase II. Neuron 20: 895-904.

58. Davis S, Laroche S (2006) Mitogen-activated protein kinase/extracellular regulated kinase signalling and memory stabilization: a review. Genes Brain Behav 5 Suppl 2: 61-72.

59. Brenman JE, Chao DS, Gee SH, McGee AW, Craven SE, et al. (1996) Interaction of nitric oxide synthase with the postsynaptic density protein PSD-95 and alpha1-syntrophin mediated by PDZ domains. Cell 84: 757-767.

60. Brenman JE, Christopherson KS, Craven SE, McGee AW, Bredt DS (1996) Cloning and characterization of postsynaptic density 93, a nitric oxide synthase interacting protein. J Neurosci 16: 7407-7415.

61. Lipton SA, Choi YB, Pan ZH, Lei SZ, Chen HS, et al. (1993) A redox-based mechanism for the neuroprotective and neurodestructive effects of nitric oxide and related nitroso-compounds. Nature 364: 626-632.

62. Fang M, Jaffrey SR, Sawa A, Ye K, Luo X, et al. (2000) Dexras1: a G protein specifically coupled to neuronal nitric oxide synthase via CAPON. Neuron 28: 183-193.

63. Kemppainen RJ, Behrend EN (1998) Dexamethasone rapidly induces a novel ras superfamily member-related gene in AtT-20 cells. J Biol Chem 273: 3129-3131.

64. Blumer JB, Cismowski MJ, Sato M, Lanier SM (2005) AGS proteins: receptor-independent activators of G-protein signaling. Trends Pharmacol Sci 26: 470-476.

65. Cismowski MJ, Ma C, Ribas C, Xie X, Spruyt M, et al. (2000) Activation of heterotrimeric G-protein signaling by a ras-related protein. Implications for signal integration. J Biol Chem 275: 23421-23424.

66. Cismowski MJ, Takesono A, Bernard ML, Duzic E, Lanier SM (2001) Receptor-independent activators of heterotrimeric G-proteins. Life Sci 68: 2301-2308.

67. Graham TE, Prossnitz ER, Dorin RI (2002) Dexras1/AGS-1 inhibits signal transduction from the Gi-coupled formyl peptide receptor to Erk-1/2 MAP kinases. J Biol Chem 277: 10876-10882.

68. Hess DT, Matsumoto A, Kim SO, Marshall HE, Stamler JS (2005) Protein S-nitrosylation: purview and parameters. Nat Rev Mol Cell Biol 6: 150-166.

69. Wang B, Feng WY, Zhu MT, Wang Y, Wang M, et al. (2009) Neurotoxicity of low-dose repeatedly intranasal instillation of nano- and submicron-sized ferric oxide particles in mice. J Nanopart Res 11: 41-53.

70. Stoltzfus RJ (2001) Iron-deficiency anemia: reexamining the nature and magnitude of the public health problem. Summary: implications for research and programs. J Nutr 131: 697S-700S.